

Recoil measurement of the $^{12}\text{C}(\pi^\pm, \pi\text{N})^{11}\text{C}$ reaction between 90 and 350 MeV

N. T. Porile

Department of Chemistry, Purdue University, West Lafayette, Indiana 47907

A. A. Caretto

Department of Chemistry, Carnegie-Mellon University, Pittsburgh, Pennsylvania 15213

B. J. Dropesky, C. J. Orth, L. C. Liu, and G. C. Giesler

Los Alamos National Laboratory, Los Alamos, New Mexico 87545

(Received 12 December 1983)

The effective forward, perpendicular, and backward ranges of ^{11}C produced in the interaction of 90–350 MeV π^\pm with carbon have been measured using conventional thick-target thick-catcher activation techniques. With increasing pion energy, the forward ranges decrease, the backward ranges increase, and the perpendicular ranges remain essentially unchanged. However, these trends are much more pronounced for π^- than for π^+ . The results have been compared with an intranuclear cascade code. The ratios of calculated effective ranges for π^- and π^+ bombardment show the same energy dependence as observed experimentally.

I. INTRODUCTION

The study of the pion-nucleon knockout reactions, $^{12}\text{C}(\pi^\pm, \pi\text{N})^{11}\text{C}$ has attracted a great deal of both theoretical and experimental interest. The excitation functions of these reactions mirror those of the free pion-nucleon interaction.^{1,2} It was therefore believed that the ratio of cross sections obtained in π^- and π^+ reactions, σ^-/σ^+ , should display a similar value at the (3,3) resonance as the free-particle pion-nucleon cross sections, i.e., three. By contrast, the experimental value of this ratio is 1.59 ± 0.07 (Ref. 2). Monte Carlo intranuclear cascade (INC) calculations with the ISOBAR code,³ which assumes quasifree dynamics and takes into account Fermi motion, Pauli blocking, final-state interactions, etc., predict $\sigma^-/\sigma^+ = 2.4$ for ^{12}C at the resonance.⁴

There have been efforts^{5–8} to explain the observed cross section ratio by supplementing quasifree knockout with final-state nucleon charge exchange (FSNCX). Despite the differences in these theoretical approaches, all these calculations indicate that final-state nucleon charge exchange plays a significant role in lowering calculated ratios.

In view of the success of these theoretical models to account for the observed σ^-/σ^+ ratio, we believe that it is of importance to examine the nature of the reaction kinematics of $(\pi, \pi\text{N})$ reactions in the presence of the (3,3) resonance and the FSNCX process. A feasible approach to this study is to measure the recoil characteristics of the residual nuclei for the $^{12}\text{C}(\pi^\pm, \pi\text{N})^{11}\text{C}$ reactions between 90 and 350 MeV. In the present work, we employ a technique that has been successfully exploited in the study of the $^{12}\text{C}(p, \text{pn})^{11}\text{C}$ reaction, namely, the measurement of thick-target recoil ranges.^{9–11} The comparison of effective recoil ranges obtained in our measurements and those

predicted by the INC calculations should indicate the adequacy of quasifree reaction kinematics.

II. EXPERIMENTAL

The experiment involved irradiations of target-catcher stacks with pions followed by assay of the induced ^{11}C activity. The irradiations were performed at the P^3 and LEP channels of the Clinton P. Anderson Meson Physics Facility (LAMPF). The π^+ and π^- energies ranged from 90 to 350 MeV, and the exposures had a duration of approximately 30 min.

The target stacks consisted of a 14.3 mg/cm^2 thick graphite foil sandwiched between two $25 \mu\text{m}$ (5 mg/cm^2) thick beryllium foils of the highest available purity. An additional Be foil was incorporated in the stack in order to permit a determination of the contribution to the observed ^{11}C activity in the catchers from reactions with impurities in the beryllium. Beryllium guard foils protected the stack from externally produced ^{11}C recoils. The target stack was irradiated in two different orientations to the beam at each energy. In experiments designed to yield the effective forward and backward ranges, the stack was mounted perpendicular to the beam direction, while in those designed to yield the perpendicular ranges, it was mounted at 10° to the beam.

Following each irradiation, the activity in the various foils was assayed with a $\gamma\text{-}\gamma$ coincidence counter consisting of two NaI(Tl) scintillation detectors mounted on either side of the foil. Windows were set on the 511-keV quanta resulting from positron annihilation in copper absorbers surrounding the foils. The various samples were counted for 1–2 h periods and decay curves were consistent with the 20.4 min half-life of ^{11}C , present in almost all instances as a single component.

TABLE I. Effective ranges of ^{11}C produced in the $^{12}\text{C}(\pi^\pm, \pi\text{N})$ reaction.

Projectile	T (MeV)	FW ($\mu\text{g}/\text{cm}^2$)	PW ($\mu\text{g}/\text{cm}^2$)	BW ($\mu\text{g}/\text{cm}^2$)
π^+	90	260 ± 13	92.0 ± 4.8	36.6 ± 11.2
	140	235 ± 13	106 ± 6	42.4 ± 3.9
	180	191 ± 10	101 ± 5	40.7 ± 3.6
	230	171 ± 9	101 ± 5	47.1 ± 3.4
	300	156 ± 8	103 ± 5	59.1 ± 4.2
	350	172 ± 9	112 ± 6	54.5 ± 3.9
π^-	90	215 ± 20	83.2 ± 4.8	17.0 ± 7.0
	140	209 ± 12	96.4 ± 4.9	30.8 ± 3.9
	180	161 ± 10	98.2 ± 4.8	37.6 ± 3.8
	230	124 ± 7	90.6 ± 4.3	51.9 ± 4.0
	300	97.7 ± 6.6	94.8 ± 4.6	72.4 ± 5.1
	350	88.7 ± 10.7	94.4 ± 5.4	70.1 ± 9.0

The contribution of the blank was found to be a significant correction, particularly for the backward catcher, where it amounted to $\sim 10\%$ at the higher energies and to as much as 40% at the lowest energy. A 5–10% correction for this effect was applied to the activity of the forward catcher as well as to that of the catchers in the 10° experiments.

III. RESULTS

The disintegration rates of the target and catcher foils were used to obtain the effective forward, backward, and perpendicular ranges of ^{11}C in carbon, designated FW , BW , and PW , respectively. The quantities F , B , and P are the fractions of the number of ^{11}C nuclei recoiling into the forward, backward, and perpendicular catchers, respectively, and W is the areal density of the target. In the case of the 10° runs, the value of P represents the average of the results obtained for the two catchers.

The results are summarized in Table I. The tabulated

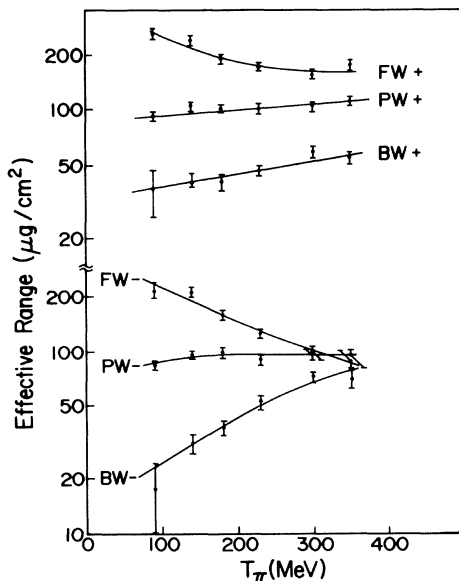


FIG. 1. Energy dependence of the effective ranges of ^{11}C from the $^{12}\text{C}(\pi^\pm, \pi\text{N})$ reaction. Top, incident π^+ ; bottom, π^- . Solid curves are drawn to guide the eye.

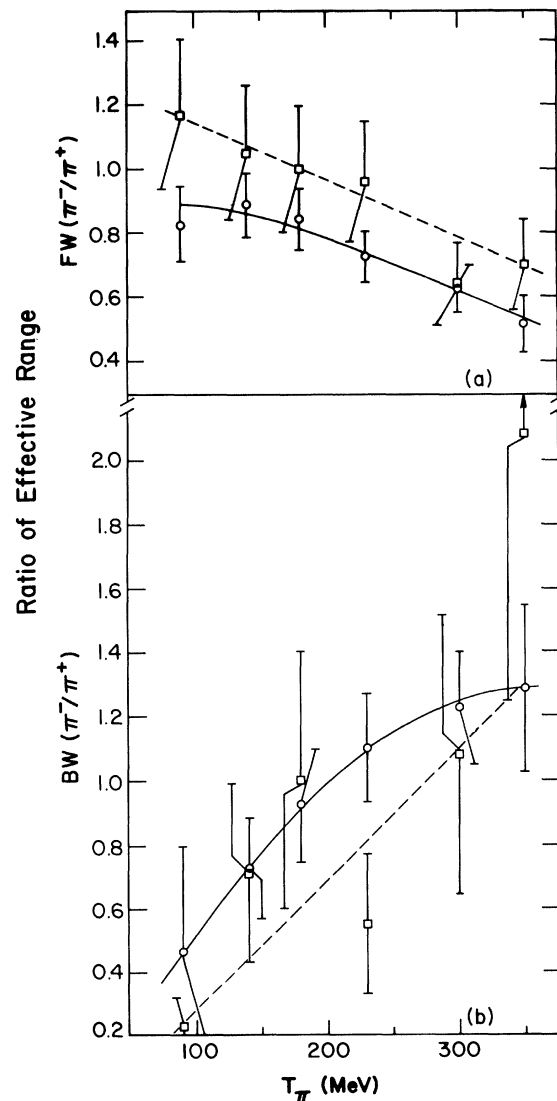


FIG. 2. Energy dependence of the ratio of effective ranges of ^{11}C produced by π^- and π^+ reactions on ^{12}C , with (a) showing $FW(\pi^-/\pi^+)$ and (b) showing $BW(\pi^-/\pi^+)$. \circ , experiment; \square , ISOBAR calculation; the solid curves (hand drawn) and dashed lines (least-squares fits) show the trends in the experimental and calculated ratios, respectively.

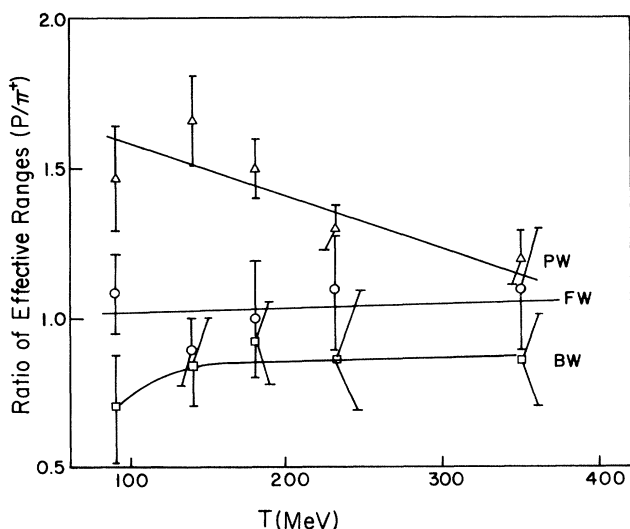


FIG. 3. Energy dependence of the ratio of effective ranges of ^{11}C formed in (p,pn) and $(\pi^+, \pi\text{N})$ reactions. The proton data are from Refs. 9–11. \circ , FW ; Δ , PW ; \square , BW . Solid curves are drawn to guide the eye.

uncertainties are based on the statistical errors, those associated with the blank correction, and the uncertainty in target thickness (3%), combined in quadrature. The overall uncertainties range from approximately 5% to as high as 40% for BW in the 90 MeV π^- experiment. Replicate experiments performed with 90 MeV π^+ agreed to within the value expected from the estimated uncertainties.

The energy dependence of the effective ranges is displayed in Fig. 1. One observes that the effective forward ranges decrease with increasing pion energy, the effective perpendicular ranges are independent of energy, and the effective backward ranges increase with bombarding energy. Furthermore, the energy dependence of FW and BW is markedly stronger for incident π^- than for π^+ . This difference is more dramatically demonstrated in Fig. 2, in which the ratios of π^- to π^+ effective ranges are plotted versus incident pion energy. As can be seen, both the FW and BW ratios exhibit large, albeit opposite, changes with energy. The significance of these trends and a comparison with similar trends predicted by ISOBAR INC calculations are considered in the next section.

Although our results constitute the first determination of recoil ranges of $(\pi, \pi\text{N})$ reaction products, similar results have been previously obtained for the $^{12}\text{C}(p, pn)$ reaction induced by protons of comparable energy.^{9–11} Figure 3 shows the ratios of effective ranges obtained with protons and π^+ as a function of bombarding energy. Within the limits of uncertainty, the FW and BW ratios are equal to unity at essentially all energies, but the values of PW are significantly larger in the proton reaction, particularly at the lower energies.

IV. DISCUSSION

Effective ranges were obtained from the ISOBAR (Refs. 3 and 4) INC calculations for comparison with the data.

The procedure followed was essentially the same as that previously described in a study of the $^{12}\text{C}(p, pn)$ recoil ranges.¹¹ Between 5 000 and 10 000 cascades were run at each experimentally studied energy for both π^+ and π^- . For each cascade resulting in a ^{11}C product, the recoil momentum was obtained from the overall energy-momentum conservation. An experimentally determined range-energy relation for ^{11}C in carbon¹¹ was used to obtain the recoil range. This quantity was then projected along an axis parallel or antiparallel to the beam depending on whether the recoil was directed into the forward or backward hemisphere, respectively, as well as along an axis perpendicular to the beam direction. The projections obtained for all the cascades that were run for a particular pion energy were then combined in the manner discussed elsewhere¹¹ for comparison with the data. The number of cascades leading to ^{11}C formation as a result of pion inelastic scattering followed by evaporation were negligibly small and were ignored.

It is most meaningful to present the results of the calculation in terms of the ratio of projected ranges obtained in π^- and π^+ reactions (Fig. 2). This procedure reduces the uncertainties associated with the conversion from recoil energy to range and permits one to focus on the physics of the reaction. The generally good agreement between the calculated and experimental ratios indicates that the ISOBAR code contains the important physics. Let us examine which factors might be responsible for the observed energy dependence of the ratios of projected ranges.

It is convenient to consider first the simplest case, in which the pion knocks out a nucleon at the first collision and the outgoing pion and nucleon do not undergo any further collisions. In this single-collision picture, if we further assume that the $(A-1)$ residual nucleus is only a spectator (the quasifree model), then the recoil momentum of the residual nucleus \vec{p}_R in the laboratory will be equal and opposite to the nucleon momentum \vec{p}_N prior to its collision with the pion, $\vec{p}_R = -\vec{p}_N$. Since \vec{p}_N is distributed isotropically in space, then, if the pion-nucleon interaction did not have a resonance (i.e., if it were independent of the collision energy), this single-collision quasifree picture of the reaction would yield the following: (a) an equality between the forward and backward recoil of the residual nucleus; and (b) an insensitivity of the recoil momentum to the incoming pion energy. Owing to the presence of the (3,3) resonance, the above phenomena are not observed. Instead, the geometry in which the pion interacts with a nucleon having an appropriate momentum for forming the (3,3) resonance will be greatly favored. If we denote the total collision energy in the c.m. frame of the πN system by W , then

$$W = \{ [E_\pi(k_0) + E_N(p_N) - B]^2 - (\vec{k}_0 + \vec{p}_N)^2 \}^{1/2},$$

or, using $\vec{p}_N = -\vec{p}_R$,

$$W = \{ m_\pi^2 + m_N^2 + 2E_\pi(k_0)E_N(p_R) + 2k_0p_R \cos\theta_R - 2B[E_\pi(k_0) + E_N(p_R) - B/2] \}^{1/2},$$

where \vec{k}_0 is the pion beam momentum, the m 's and E 's are, respectively, the masses and energies of the particles, and B is the binding energy of the ejected nucleon. The

θ_R is the recoil angle with respect to the direction of \vec{k}_0 . Consequently, forward and backward recoils correspond to $\cos\theta_R > 0$ and < 0 , respectively. From this last equation, we see that for pions with incoming energies below ~ 180 MeV, the (3,3) resonance energy ($W = 1232$ MeV) is easily reached with the geometry having $p_R \cos\theta_R > 0$; that is, with the collision associated with a target nucleon moving toward the incoming pion. This situation also corresponds to an enhanced probability of observing forward recoils. Furthermore, the lower the pion energy, the larger will be the forward recoil momentum compared with the backward recoil momentum. The situation is reversed for pion energies higher than ~ 180 MeV. The resonance energy is more easily reached with $p_R \cos\theta_R < 0$, corresponding to a nucleon moving in the same direction as the incoming pion. The higher the pion energy, the smaller will be the forward recoil momentum and the larger will be the backward recoil momentum. Thus, this single-collision quasifree picture is already able to describe the general trend of the observed recoil momenta, namely, that the forward recoil decreases with pion energies while the backward recoil increases.

In the present $^{12}\text{C}(\pi^\pm, \pi\text{N})^{11}\text{C}$ study, the leading contributions to the production of ^{11}C come from the basic $\pi^\pm\text{n}$ scatterings. In π^-n scattering the resonating P_{33} -wave component is more dominant against the nonresonating background than in π^+n scattering. Consequently, we have for the $^{12}\text{C}(\pi^+, \pi\text{N})^{11}\text{C}$ reaction a situation closer to the ideal nonresonance situation discussed in the last paragraph. This explains why the energy dependence of the observed FW and BW recoil is less prominent for the $^{12}\text{C}(\pi^+, \pi\text{N})^{11}\text{C}$ reaction than for the $^{12}\text{C}(\pi^-, \pi\text{N})^{11}\text{C}$ reaction and accounts for the variation with energy of the ratio of ranges. It also accounts for the similarity between $(\pi^+, \pi\text{N})$ and (p, pn) reactions (Fig. 3). The real situation is, of course, more complex in that multiple collisions are important. For example, a pion can lose energy through collisions before the one that knocks out a nucleon so that the effective pion energy for the last πN collision is much lower than the beam energy. This possibility has been fully taken into account by our INC calculations.

In summary, the comparison of the recoil characteristics of the reaction product ^{11}C from the $(\pi^\pm, \pi\text{N})$ reactions in ^{12}C with those from the (p, pn) reaction shows the important role of the (3,3) resonance in the kinematics of the pion reactions. The qualitative agreement between our experimental data and INC calculations indicates that the kinematics for the $^{12}\text{C}(\pi^\pm, \pi\text{N})^{11}\text{C}$ reactions is basically governed by multiple quasifree scattering and seems insensitive to FSNCX details. This insensitivity can be understood if one recalls that contributions to (p, n) -type nucleon charge exchange come mainly from the small-angle scattering region, where the momentum transfer given to the residual nucleus is small. Consequently, although FSNCX can have large effects on cross sections and on the ratio of the latter, it can only alter slightly the quasifree feature of recoil characteristics. We should note, however, that the INC model makes use of free πN and NN cross sections and is classical in the sense that interference effects between multiple scattering and FSNCX processes leading to the same final state are absent in the model. Since the interference effects are by no means negligible,⁸ the lack of such effects in the INC model could be the origin of the quantitative discrepancy between INC calculations and the measurements as shown in Fig. 2.

V. CONCLUSIONS

The effective forward, perpendicular, and backward recoil ranges of ^{11}C produced in the interaction of 90–350 MeV π^\pm with ^{12}C have been measured. Sizable differences in the energy dependence of the ranges determined for π^+ and π^- are seen. These differences can be accounted for by the ISOBAR intranuclear cascade code, and can be understood in terms of the larger amplitudes of the π^-n than for the π^+n scattering at the collision energy corresponding to the (3,3) resonance.

This work was supported by the U. S. Department of Energy.

¹P. L. Reeder and S. S. Markowitz, Phys. Rev. **133**, B639 (1964).

²B. J. Dropesky, G. W. Butler, C. J. Orth, R. A. Williams, M. A. Yates-Williams, G. Friedlander, and S. B. Kaufman, Phys. Rev. C **20**, 1844 (1979).

³G. D. Harp, K. Chen, G. Friedlander, Z. Fraenkel, and J. M. Miller, Phys. Rev. C **8**, 581 (1973); J. N. Ginocchio, *ibid.* **17**, 195 (1978).

⁴In the original ISOBAR model, the analog nucleon-nucleus charge exchange is prohibited. We have found that the removal of this restriction has a small numerical effect on the calculated cross sections.

⁵P. W. Hewson, Nucl. Phys. **A133**, 659 (1969).

⁶M. M. Sternheim and R. R. Silbar, Phys. Rev. Lett. **34**, 824 (1975).

⁷Y. Ohkubo and N. T. Porile, Phys. Rev. C **25**, 2638 (1982).

⁸Y. Ohkubo and L.-C. Liu, private communication indicating new model calculations show that the interference effects between quasifree scattering and nucleon charge exchange, rather than the nucleon charge exchange itself, are largely responsible for the observed low σ^-/σ^+ ratio, Los Alamos National Laboratory, Isotope and Nuclear Chemistry Division Annual Report No. FY 1983, 1983.

⁹S. Singh and J. M. Alexander, Phys. Rev. **128**, 711 (1962).

¹⁰S. Hontzeas, Can. J. Chem. **46**, 267 (1968).

¹¹N. T. Porile, Nucl. Phys. **A130**, 88 (1969).